

# Anomalous effects in interacting spinless fermion systems with local disorder

R Vlaming, G S Uhrig and D Vollhardt

Institut für Theoretische Physik C, Technische Hochschule Aachen, D-5100 Aachen,  
Federal Republic of Germany

**Abstract.** Spinless fermions with local disorder and nearest neighbour repulsion are investigated on a Bethe lattice with infinite branching. Two phases are studied: a homogeneous phase and a checkerboard charge-density wave. Within this framework the model is exactly solved for all values of disorder, interaction and temperature. The transition between the two phases is described in detail. The density of states  $\rho(\omega)$ , critical interaction  $U_c$  and order parameter  $b$  are calculated. The system displays anomalous behaviour: away from half-filling particle-density fluctuations due to weak disorder and/or low temperatures favour spontaneous symmetry breaking. We analyse and explain this unconventional phenomenon.

## 1. Introduction

One of the most important objectives of condensed matter theory is to reach a proper understanding of correlated, i.e. interacting and/or disordered, fermionic systems. Taken separately, correlation effects due to interaction and disorder already lead to highly complicated problems. Their simultaneous presence naturally gives rise to even more subtle effects. The majority of recent investigations of interacting disordered electron systems are based on the theory developed for the Anderson localization problem, i.e. for disordered systems without interactions [1]. In this theory the initial problem is mapped onto a field theory [2], which is investigated by renormalization group techniques. A generalization of this approach to the case of disordered electrons [3] in the presence of interactions subsequently led to considerable insight into the problem [4]; for a review see [1]. The formation of local magnetic moments, which leads to serious complications in the application of the renormalization group, was first recognized by Finkel'shtein [5] and Castellani *et al* [6] in the framework of a continuum model with disorder, and further developed in [7, 8]. In the framework of a Hubbard model with local disorder it was discussed in [9]. The latter model was also used by Ma [10] to study the phase diagram by means of a real-space renormalization group. Its strong coupling version, i.e. the  $t$ - $J$  model with disorder, was investigated by Zimanyi and Abrahams [11].

To gain a better understanding of the full interplay between disorder and interaction effects an exactly solvable itinerant quantum model is desirable. Since such a model is not available in finite dimensions  $d > 1$  one would, at least, like to construct a comprehensive mean-field theory which is valid for all input parameters,

i.e. interaction, disorder, temperature, particle density, etc. Such a mean-field theory is, for example, provided by the solution of a lattice model in the limit of high dimensions or coordination number  $Z$ . This approach, which is well established in classical statistical mechanics, has also recently been formulated for quantum mechanical lattice models with itinerant degrees of freedom [12]. In the limit  $Z \rightarrow \infty$  microscopic many-body methods are greatly simplified, without becoming trivial (for reviews, see [13, 14]). In particular, one can show [15] that (i) the 'coherent potential approximation' becomes the exact solution for the Anderson disorder model, and (ii) in the case of interacting systems with a Hubbard-type Hamiltonian (without disorder) only the Hubbard interaction remains dynamical, while all other interactions (e.g. nearest neighbour interaction) reduce to their Hartree substitute [16]. Indeed, in the limit  $Z \rightarrow \infty$  the problem of interacting systems with Hubbard interaction becomes a dynamical single-site theory [17, 18] which may be exactly formulated in terms of a generalized coherent potential [17, 19].

As stated above it is our aim to study the interplay of disorder and interaction for the full range of parameters by means of the limit  $Z \rightarrow \infty$ . Since the Hubbard model, even without disorder, remains very complicated in this limit it is not the right candidate. Therefore, we choose to examine a model of spinless fermions with nearest neighbour interaction and site-diagonal disorder. In this model we know the solutions of the limits of zero disorder and zero interaction, respectively. The model is indeed exactly solvable in the limit  $Z \rightarrow \infty$  for all disorder and interaction strengths. This enables us to calculate all relevant physical quantities, such as the density of states, critical interaction, and so on, *explicitly*. The use of  $Z \rightarrow \infty$  as an approximation of a finite-dimensional system has the advantage of treating disorder *and* interaction on an equal footing. The arbitrariness, which enters when two or more expansions are used, e.g. in the disorder *and* in the interaction or in the disorder *and* in  $\epsilon = d - 2$ , is ruled out since only *one* approximation step is involved. It is controlled by the small parameter  $1/Z$  so that systematic corrections are possible.

A model of interacting fermions without spin degeneracy may be useful in the case of strongly polarized systems (e.g. in a lattice-gas description of  $^3\text{He}$  in a strong magnetic field), as well as ferromagnetic (or ferrimagnetic) electronic systems where, for example, the down-spin bands are filled and only an up-spin band needs to be considered. The latter situation is realized in magnetite ( $\text{Fe}_3\text{O}_4$ ), where the lowest singlet spin-up band is half filled, leading to metallic conductivity above a temperature  $T_v \simeq 119\text{ K}$  at atmospheric pressure. At  $T_v$  the system undergoes the Verwey transition into an insulator [20]. Cullen and Callen [21, 22] first suggested a model of spinless fermions with nearest neighbour interaction without disorder to describe this transition.

The model itself can be solved exactly in  $d = 1$  [23, 24]. In  $d = 1$  and for half filling the solution describes a transition from a homogeneous to a charge-density-ordered phase *at a finite value of the interaction*. This is also borne out in a variational treatment, using a Gutzwiller wavefunction plus Gutzwiller approximation [25]. The transition was discussed in detail by Shankar [26], who also calculated various response functions and gave a qualitative argument concerning the effect of disorder on the transition. According to his argument arbitrarily weak disorder will destroy the interaction-induced energy gap. A transition to a charge-density-ordered state at a finite interaction turns out to be a peculiarity of the dimension  $d = 1$  [27].

For  $d > 1$  and half filling on a bipartite lattice the transition is shifted to arbitrarily small interactions, as may be expected from the perfect-nesting property.

This is important for our investigation since the Hartree solution of the model without disorder (which becomes exact for  $Z \rightarrow \infty$ ) also has this feature. A straightforward generalization of Shankar's disorder argument to higher coordination numbers reveals that a non-trivial competition between interaction and disorder is present for  $d \geq 2$ . Hence, the mean-field solution already correctly describes two important aspects of the exact solution in finite dimensions  $d = 2, 3$ , at least qualitatively.

The paper is organized as follows. The model and details of the perturbational treatment are given in section 2. In sections 3 and 4 our results for the density of states and the phase transition line critical interaction against filling are shown. We interpret our findings in section 5. In section 6 the critical behaviour across the phase transition is examined while the discussion in section 7 concludes the main part of our article.

## 2. Model

The basis of our investigations is a tight-binding Hamiltonian for spinless fermions with nearest neighbour hopping, local disorder and nearest neighbour repulsion (screened Coulomb interaction)

$$\hat{H} = \sum_i (\epsilon_i - \mu) \hat{n}_i + \sum_{i,j} t_{ij} \hat{c}_i^\dagger \hat{c}_j + \frac{1}{2} \sum_{i,j} U_{ij} \hat{n}_i \hat{n}_j \quad (1)$$

where  $\hat{c}_i^\dagger$  ( $\hat{c}_i$ ) are the creation (destruction) operators for fermions on site  $i$ ,  $\hat{n}_i = \hat{c}_i^\dagger \hat{c}_i$  and  $U_{ij}, t_{ij} = 0$  if  $i, j$  are not nearest neighbours. For the model to remain non-trivial in the limit of high coordination numbers,  $Z \rightarrow \infty$ , the hopping matrix elements and the interaction matrix elements are scaled as  $t_{ij} := -t/\sqrt{Z}$  and  $U_{ij} := U/Z$ , respectively [12, 16]. The energy  $\epsilon_i$  is a stochastic variable drawn from some local, site-independent distribution function  $P(\epsilon)$ . The chemical potential is  $\mu$ .

In our investigation we choose to work on a Bethe lattice with branching  $K = Z - 1$ . This has the advantage that in the limit  $K \rightarrow \infty$  the density of states is exactly given by a half ellipse, whereby explicit analytic calculations are made possible [15, 28]. In the case of the one-particle quantities to be calculated below, the peculiar properties of the Bethe lattice (absence of loops, etc) do not lead to unphysical features. The most important aspect of the lattice in the correlation problem under investigation, namely the bipartite structure, is equally provided by the Bethe lattice.

To tackle the problem set out above we will proceed as follows. First, an equation of motion is constructed using Green functions in a locator representation. Then, writing the space-diagonal Green function (full locator) in terms of a renormalized perturbation expansion, the limit of large branching is taken. Finally, we formally resum the diagrammatic series to obtain a closed system of equations. Throughout this paper we will work in units of  $\hbar = 1$ ,  $k_B = 1$  and  $t/\sqrt{K} = 1$ .

### 2.1. Perturbation technique for $K \rightarrow \infty$

The one- and two-particle imaginary-time Green functions are defined by

$$G(i, \tau_i; j, \tau_j) = -\langle T \hat{c}_i(\tau_i) \hat{c}_j^\dagger(\tau_j) \rangle \quad (2a)$$

$$G(i, \tau_i; n, \tau_n; j, \tau_j; m, \tau_m) = -\langle T \hat{c}_i(\tau_i) \hat{c}_n(\tau_n) \hat{c}_j^\dagger(\tau_j) \hat{c}_m^\dagger(\tau_m) \rangle. \quad (2b)$$

Here  $\langle \rangle$  indicates the quantum mechanical ensemble average at finite temperature. The ensemble average with respect to the disorder of some physical quantity  $X$  is given by

$$\bar{X} := \prod_i \int d\epsilon_i P(\epsilon_i) X(\epsilon_1, \dots, \epsilon_i, \dots). \quad (3)$$

Using standard techniques [29–31] an equation of motion for the Green function is obtained. With  $G_{ij}(z_l)$  and  $G_{iqjq}(z_l, z_r, z_s)$  as the Fourier transforms with respect to time of (2a) and (2b), respectively, we find

$$G_{ij}(z_l) = g_i^0(z_l)\delta_{ij} + \sum_q g_i^0(z_l)t_{iq}G_{qj}(z_l) + \sum_q \beta^{-2} \sum_{rs} g_i^0(z_l)U_{iq}G_{iqjq}(z_l, z_r, z_s) \quad (4)$$

where  $z_l = \mu + i\omega_l$  and  $\omega_l = \pi(2l + 1)/\beta$ . For the bare locator,  $g_i^0(z_l)$ , we have

$$g_i^0(z_l) = \frac{1}{z_l - \epsilon_i}. \quad (5)$$

The two-particle Green function appearing in (4) depends only on three frequencies because explicitly time-dependent fields are absent in (1). The inverse temperature is denoted by  $\beta$  and the variables  $r, s$  run over all integers. Figure 1 is the pictorial representation of (4). It illustrates how the perturbative terms (hopping, interaction) appear, and how the different frequencies  $(z_l, z_r, z_s)$  and sites  $(i, q, j)$  are related.

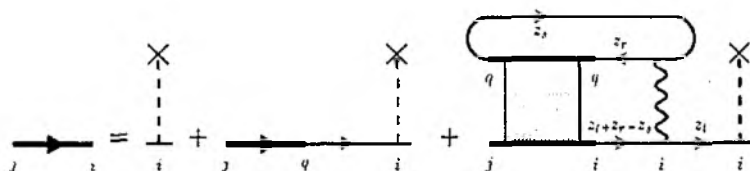


Figure 1. Diagrammatic representation of the equation of motion. One-particle Green function: fat line with full arrow; hopping amplitude: thin line with full arrow; bare locator: broken vertical line with cross; two-particle Green function: two fat lines with shaded square; nearest neighbour interaction: wavy curve.

In the same way one can construct an equation of motion for  $G_{iqjq}(z_l, z_r, z_s)$ . This equation does not contain irreducible three-particle vertices. Thus, by expansion of the latter equation and (4), the explicit perturbation expansion in terms of  $g_i^0(z_l)$ ,  $t_{ij}$  and  $U_{ij}$  is obtained. Subsequently we consider the space-diagonal element of the Green function, i.e. the ‘full locator’  $g_i(z_l) := G_{ii}(z_l)$ . For  $g_i(z_l)$  we write down an expansion in such a way that, of all perturbation terms mentioned above, those with a contribution from a given site, say  $i$ , are isolated. Formally this can be written as

$$g_i(z_l) = g_i^0(z_l) + g_i^0(z_l)\Sigma_i(z_l)g_i(z_l). \quad (6)$$

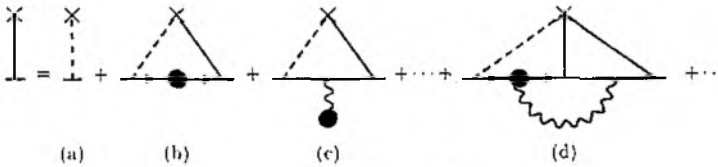


Figure 2. Expansion of the full locator (indicated by the full vertical line with a cross) in terms of the self-energy; (a) bare locator; contribution to the perturbation via (b) hopping, (c) interaction and (d) combination of hopping and interaction.

The essential point of (6) is that  $\Sigma_i(z_l)$  does not depend on  $\epsilon_i$ . An expansion of (6) is given in figure 2. In figure 2(b) two hopping amplitudes connect  $g_i^0$  with the rest of the locators; in figure 2(c) this role is played by the interaction. Finally, figure 2(d) gives an example of a combined effect.

At this point we introduce the limit of infinite branching,  $K \rightarrow \infty$ . In analogy to the simplifications for infinite dimensions discussed for nearest neighbour interactions by Müller-Hartmann [16] and for disordered systems by Vlaming and Vollhardt [15], we have a dramatic reduction of terms in the expansion (6), represented in figure 2. In fact, from the terms given in figure 2, *only* figures 2(a-c) remain. In particular, diagrams containing irreducible contributions in the disorder and the interaction, such as figure 2(d), *vanish* in the limit  $K \rightarrow \infty$ . This conclusion is apparent from figure 2. Each hopping integral contributes a factor  $K^{-1/2}$ , each interaction contributes a factor  $K^{-1}$  and each sum over free sites contributes a factor  $K$ . For the diagrams in figures 2(b, c) this results in  $K^{-1/2} K^{-1/2} K \sim 1$  and  $K^{-1} K \sim 1$ , respectively. However, figure 2(d) gives  $K^{-1/2} K^{-1/2} K^{-1} K \sim K^{-1}$ , thus it vanishes in the limit  $K \rightarrow \infty$ . From this example we learn that the self-energy  $\Sigma_i(z_l)$  decouples into *two independent contributions*. For the full locator we write

$$g_i = g_i^0 + g_i^0 \sigma_i g_i + g_i^0 s_i g_i \quad (7)$$

where the  $z_l$  dependence is suppressed for clarity. The self-energy  $\sigma_i(z_l)$  results from the perturbation in the hopping, the self-energy  $s_i$  from the perturbation in the interaction. Physically, a particle at site  $i$  is subject to two additive effective potentials, one due to the disorder, the other due to the interaction, both originating from the surrounding system. This is a typical mean-field property.

Making use of the renormalized perturbation expansion [29] for a Bethe lattice the self-energies are simply given by

$$\sigma_i(z_l) = \sum_j t_{ij} g_j^{-(i)}(z_l) t_{ij} \quad (8a)$$

$$s_i = \beta^{-1} \sum_l \sum_j U_{ij} g_j^{-(i)}(z_l). \quad (8b)$$

The superscripts representing a site with a minus sign imply that the locator does not depend on the energy of that particular site. Since in the limit  $K \rightarrow \infty$  only Hartree diagrams for the nearest neighbour interaction remain, the related self-energy,  $s_i$ , is *frequency independent*. This is an *exact*, albeit special, and highly simplifying feature of our model for  $K \rightarrow \infty$ . The equations (8) introduce a new

locator,  $g_j^{-(i)}$ , which has an expansion like (7). In such an expansion site  $i$  must be excluded everywhere, thus leading to new self-energies  $\sigma_j^{-(i)}$  and  $s_j^{-(i)}$ , etc. In the next subsection we will explain how this hierarchy of equations can be closed by averaging over the disorder.

## 2.2. Introduction of two different phases

On every bipartite lattice, i.e. a lattice of A-B structure, there are at least two possible phases depending on the interaction strength. For  $U = 0$  the system is in the homogeneous phase, which implies that the averaged full locator is site independent. On the other hand, for  $U \gg 1$  the checkerboard phase or charge density wave (CDW) is more favourable from the energetic point of view. For intermediate interaction strengths,  $U \approx 1$ , the situation is not *a priori* clear.

A part of a Bethe lattice for  $K = 2$  is shown in figure 3. It is important to recognize that in the limit  $K \rightarrow \infty$  one has  $\overline{g_i} = \overline{g_i^{-(\dots)}}$ , where  $(\dots)$  may stand for any finite number of sites [15]. This is clear in the special case  $\overline{g_i} = \overline{g_i^{-(j)}}$  because site  $j$  is only one of the  $K + 1 \rightarrow \infty$  neighbours of site  $i$ .

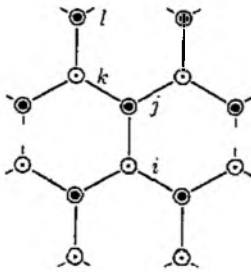


Figure 3. Part of a Bethe lattice with  $K = 2$ . Sites  $i, j, k$  and  $l$  form a path along which the local electron filling alternates. Sites  $i$  and  $k$ : low filling, and sites  $j$  and  $l$ : high filling.

Suppose the system is in a homogeneous phase at  $U = 0$ ; then we have  $\overline{g_i} = \overline{g_j}$  for all  $i, j$ . One may equally write  $\overline{g_i} = \overline{g_j^{-(i)}}$  as was illustrated above (see figure 3). The latter equation can be used directly in (8a). Averaging (7) leads to the quantities  $\overline{\sigma_i}$  and  $\overline{s_i}$ . Since the filling is kept constant the site-independent self-energy  $\overline{s_i}$  merely shifts the chemical potential, thereby ruling out any effect of the interaction. Now suppose the system is in the checkerboard phase,  $U \gg 1$ ; then all points on each of the sublattices A, B are equal, i.e.  $\overline{g_{i \in A}} = \overline{g_{k \in A}}$  and  $\overline{g_{j \in B}} = \overline{g_{l \in B}}$  (see also figure 3).

As mentioned above, for general  $U$  we do not rigorously know the structure of the most favourable phase. Since this information has to be put in *by hand*, we restrict ourselves to the simplest symmetry extension and assume a checkerboard phase. Thus we make the following ansatz:

$$g_U := \overline{g_i} = \overline{g_k^{-(j)}} = \dots \quad (9a)$$

$$g_L := \overline{g_j^{-(i)}} = \overline{g_l^{-(k)}} = \dots \quad (9b)$$

where the roman indices U (upper) and L (lower) energetically distinguish between the two sublattices. The sublattice L is that sublattice on which an electron when added to the system, has the lower interaction energy. Note that this is the sublattice with the *higher* electron filling. For sublattice U the opposite applies. In figure 3 this feature is clarified using small and big dots representing the filling at each site.

For  $g_U = g_L$  we recover the homogeneous phase and the phase with  $g_U \neq g_L$  we will simply call CDW. Equations (9) close the hierarchy indicated above, albeit on a higher level. Algebraic manipulations, making use of (7)–(9), lead to

$$\begin{aligned}
 g_U(z_l) &= \int d\epsilon_i P(\epsilon_i) \frac{g_i^0(z_l)}{1 - g_i^0(z_l)(\sigma_U(z_l) + s_U)} \\
 \sigma_U(z_l) &= g_L(z_l) \quad s_U = \frac{U}{\beta} \sum_r g_L(z_r) \\
 g_L(z_l) &= \int d\epsilon_j P(\epsilon_j) \frac{g_j^0(z_l)}{1 - g_j^0(z_l)(\sigma_L(z_l) + s_L)} \\
 \sigma_L(z_l) &= g_U(z_l) \quad s_L = \frac{U}{\beta} \sum_r g_U(z_r).
 \end{aligned} \tag{10}$$

We now switch to real frequencies  $\omega$  by analytic continuation. The filling of the upper and the lower sublattice, respectively, is given by

$$n_{U,L} := -\frac{1}{2\pi} \int_{-\infty}^{\infty} d\omega \operatorname{Im} \{g_{U,L}(\omega)\} f_F(\omega) \tag{11}$$

where  $f_F(\omega) = [\exp(\beta(\omega - \mu)) + 1]^{-1}$  is the Fermi distribution. The total filling  $n$  and the order parameter  $b$  are defined by

$$n := \frac{1}{2}(n_L + n_U) \tag{12a}$$

$$b := \frac{1}{2}(n_L - n_U). \tag{12b}$$

In the homogeneous phase we have  $b = 0$ , while in the CDW phase  $b$  may vary between 0 and  $\frac{1}{2}$ .

We now choose the disorder distribution to be semi-elliptic:

$$P(\epsilon) = \frac{1}{\pi\sqrt{\gamma}} \sqrt{1 - \epsilon^2/4\gamma} \tag{13}$$

where  $4\sqrt{\gamma}$  is the width of the distribution. The main motivation for this choice is that it contains only a single parameter and that the integrals remain tractable. Inserting (13) and (12) in (10) we obtain

$$\gamma g_U^2 - (\omega - g_L - \Delta) g_U + 1 = 0 \tag{14a}$$

$$\gamma g_L^2 - (\omega - g_U + \Delta) g_L + 1 = 0 \tag{14b}$$

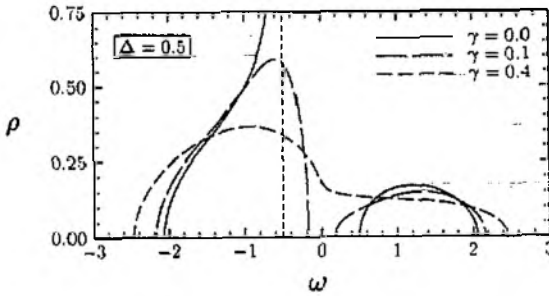


**Figure 4.** DOS in the CDW phase for  $\Delta = 0.5$ . For  $\gamma = 0$  the DOS consists of two bands, and diverges at  $\omega = -0.5$  (asymptote indicated by thin broken line). For  $\gamma = 0.1$  the band gap has become smaller and the divergence is smeared out. For  $\gamma = 0.4$  the two bands have merged.

where  $\Delta := Ub$  and the chemical potential has been renormalized as  $\mu \rightarrow \mu + Un$ . The latter merely indicates that  $\mu$  is shifted by the interaction to keep  $n$  constant. Using (12) and (11), and the definition of  $\Delta$ , one finds

$$n(\beta, \gamma) = - \int_{-\infty}^{\infty} \frac{d\omega}{2\pi} \text{Im} \{g_L(\omega) + g_U(\omega)\} f_F(\omega) \tag{15a}$$

$$U(\beta, \gamma) = -\Delta \left( \int_{-\infty}^{\infty} \frac{d\omega}{2\pi} \text{Im} \{g_L(\omega) - g_U(\omega)\} f_F(\omega) \right)^{-1}. \tag{15b}$$

For given  $\gamma$  and  $\beta$  one has to find values for  $\mu$  and  $\Delta$  such that  $n(\beta, \gamma)$  and  $U(\beta, \gamma)$  equal  $n$  and  $U$  for the system under investigation. In this sense (14) and (15) form a self-consistent system. These equations are the central ones in our paper.

### 3. Density of states

There are four different situations, depending on the values of  $\gamma$  and  $\Delta$ .

(i) For  $\gamma = 0, \Delta = 0$ , i.e. free electrons on a Bethe lattice with infinite branching, the DOS is known to be semi-elliptic [29]. This also follows from (14) which is a quadratic equation in  $g(\omega)$ , defined as

$$g(\omega) := \frac{1}{2}(g_L(\omega) + g_U(\omega)) \tag{16}$$

because  $g_U(\omega) = g_L(\omega)$ .

(ii) In the homogeneous state with finite disorder ( $\gamma \neq 0, \Delta = 0$ ) equation (14) remains quadratic in  $g(\omega)$ , but the DOS broadens by a factor  $\sqrt{1 + \gamma}$ .

(iii) In the CDW state without disorder ( $\gamma = 0$  and  $\Delta \neq 0$ ) we have  $g_U(\omega) \neq g_L(\omega)$ , but the equation for  $g(\omega)$  remains quadratic. The retarded Green function for the lower sublattice is

$$g_L(\omega) = \frac{\omega - \Delta}{2} - \frac{i}{2} \sqrt{\frac{\omega - \Delta}{\omega + \Delta} (\Delta^2 + 4 - \omega^2)} \tag{17}$$

and for the upper sublattice one has  $g_U(\omega) = g_L(\omega)|_{\Delta \rightarrow -\Delta}$ . The DOS for the lower sublattice is plotted in figure 4. It displays the existence of two bands with a bandgap of  $2\Delta$ . The bands extend from  $-\Delta$  to  $-\sqrt{\Delta^2 + 4}$  and from  $\Delta$  to  $\sqrt{\Delta^2 + 4}$  with a divergence at  $\omega = -\Delta$ .

(iv) The most complicated situation arises for the CDW state in the presence of disorder ( $\gamma \neq 0$ ,  $\Delta \neq 0$ ). Equation (14) can be rewritten as

$$[4\gamma^2(\gamma+1)]g^4(\omega) + [-4\omega\gamma(2\gamma+1)]g^3(\omega) + [4\gamma^2 + (5\omega^2 - \Delta^2)\gamma + (\omega^2 - \Delta^2)]g^2(\omega) + [\omega(\Delta^2 - \omega^2 - 4\gamma)]g(\omega) + \omega^2 = 0 \quad (18a)$$

$$\frac{1}{2}(g_L(\omega) - g_U(\omega)) = -\frac{g(\omega)\Delta}{\omega - 2\gamma g(\omega)}. \quad (18b)$$

Equation (18) provides the overall DOS, while the DOS of the sublattices is found from (18b). Although (18a) allows for several complex solutions the requirement  $\text{Im}\{g_L(\omega)\} \leq 0$  and  $\text{Im}\{g_U(\omega)\} \leq 0$  determines a unique solution for any allowed  $\omega, \gamma$  and  $\Delta$ . In figure 4 the DOS for the lower sublattice is plotted for  $\Delta = 0.5$  with  $\gamma = 0.1$  and  $\gamma = 0.4$ , respectively. The divergence at  $\omega = -\Delta$  disappears for finite  $\gamma$ . For larger values of  $\gamma$  the two subbands merge. The symmetry of  $g(\omega)$ ; i.e.  $g(-\omega) = g(\omega)$ , implies that the bands merge at  $\omega = 0$ . To find the critical value  $\Delta_c$  for which  $\Delta$  the bands merge the solutions of (18a) have to be examined for  $\omega = 0$ . One finds

$$\Delta_c = \frac{2\gamma}{\sqrt{\gamma+1}}. \quad (19)$$

The existence of such a critical  $\Delta$  can be understood as follows. A strong interaction leads to a phase transition from the homogeneous phase to the CDW; the larger  $U$  is, the bigger the energy difference between the bands will be. On the other hand, disorder generally leads to broadening of a band, so that, if the disorder is large enough, the zero-energy states are accessible for the electrons. These effects compete so that a critical  $\Delta$ , which depends monotonically on the disorder, must exist.

#### 4. The phase transition line

In this paragraph we determine in the critical interaction value  $U_c$  for which the phase transition appears.  $U_c$  depends on the disorder, the temperature and, through the chemical potential  $\mu$ , on the filling. By taking  $\Delta \rightarrow 0$  in (14) and (15) one finds

$$n(\beta, \gamma) = \int_{-2\sqrt{\gamma+1}}^{2\sqrt{\gamma+1}} \frac{d\omega}{2\pi} \frac{\sqrt{4(\gamma+1) - \omega^2}}{\gamma+1} f_F(\omega) \quad (20a)$$

$$U_c(\beta, \gamma) = \left( \int_{-2\sqrt{\gamma+1}}^{2\sqrt{\gamma+1}} \frac{d\omega}{2\pi} \frac{\omega \sqrt{4(\gamma+1) - \omega^2}}{\omega^2(\gamma-1) - 4\gamma^2} f_F(\omega) \right)^{-1}. \quad (20b)$$

In the subsequent subsections we shall discuss (20) for different values of  $\beta$  and  $\gamma$ . Furthermore, the case of half filling and the empty band limit will be investigated.

#### 4.1. Zero temperature and finite disorder

In the limit of zero temperature,  $\beta \rightarrow \infty$ , explicit integration of (20) is possible and we obtain

$$n(\infty, \gamma) = \frac{\mu}{2\pi(\gamma+1)} \sqrt{4(\gamma+1) - \mu^2} + \frac{1}{\pi} \cos^{-1}\left(-\frac{\mu}{2\sqrt{\gamma+1}}\right) \quad (21a)$$

$$U_c(\infty, \gamma) = 2\pi\{[4(1+\gamma) - \mu^2]^{3/2} H_1(\mu, \gamma)\}^{-1} \quad (21b)$$

where we made use of an auxiliary function:

$$H_1(\mu, \gamma) := \begin{cases} -1/h^2 + (1/h^3) \ln[(2+h)/(2-h)] & \gamma < 1 \\ \frac{1}{12} & \gamma = 1 \\ 1/h^2 - (2/h^3) \tan^{-1}(\frac{1}{2}h) & \gamma > 1 \end{cases} \quad (22a)$$

$$h := [1 - \gamma(4(1+\gamma) - \mu^2)]^{1/2}. \quad (22b)$$

The Fermi level must fulfill the constraint  $|\mu| \leq 2\sqrt{\gamma+1}$ . In figure 5  $U_c$  is plotted against  $n$  for different values of the disorder. For vanishing disorder the logarithmic term  $\ln(2 - \sqrt{4 - \mu^2})$  remains so that the behaviour at  $\mu \rightarrow 0$ , i.e. at half filling, is singular. This is the so-called perfect-nesting singularity, which results from the lattice being bipartite. Away from half filling it disappears like  $U_c \sim -\pi/[\ln(\pi(n - \frac{1}{2})/4) + 1]$ . In the same way this divergence disappears if the disorder is small (but finite), namely like  $U_c \sim -\pi/[\ln(\gamma/2) + 1]$ .

In figure 5 several interesting effects of the disorder can be observed. Comparing the curve for  $\gamma = 0$  with  $\gamma = 0.1$  we see that they intersect for  $n \approx 0.43$ . Qualitatively, this holds for any two curves with different disorder strength. To describe this phenomenon we introduce the filling  $n_A(\gamma)$  at which two  $U_c$  against  $n$  curves, which differ only by  $d\gamma$  in the disorder, intersect. From figure 5 we learn that by varying  $\gamma \rightarrow \gamma + d\gamma$  at filling  $n < n_A(\gamma)$  the critical interaction  $U_c$  decreases, whereas at filling  $n > n_A(\gamma)$  an increase of  $U_c$  occurs. The behaviour in the region  $n < n_A(\gamma)$  may be called 'anomalous' (compared with the conventional situation) because the disorder favours the CDW phase in this region. Thus  $n_A(\gamma)$  is the filling that separates anomalous from conventional disorder dependence. For increasing disorder  $n_A(\gamma)$  decreases so that the anomalous region becomes smaller. A detailed investigation of the latter observation is given in appendix A.

An explicit example may shed some light on this unusual behaviour. Let us consider a system that has a filling  $n^*$  and an interaction  $U^*$  as indicated in figure 5. In a sample with low disorder this system is in the homogeneous phase. If the disorder is somewhat stronger,  $\gamma \approx 0.1$ , the system displays a CDW structure and for a strongly disordered system,  $\gamma \geq 0.5$ , the system is in the homogeneous phase again. Reappearance of the homogeneous phase is not surprising because for strongly disordered systems the disorder dominates. Thus, for any (finite) filling  $n > n_A$ , a certain value of the disorder exists from which on the  $U_c$  against  $n$  curves are 'ordered', i.e.  $U_c(\infty, \gamma_1) > U_c(\infty, \gamma_2)$  if  $\gamma_1 > \gamma_2$ .

#### 4.2. Finite temperature and zero disorder

In figure 6  $U_c$  is plotted against  $n$  for various values of the temperature at zero disorder ( $\gamma = 0$ ). In the limit  $\beta = \infty$  we recover the curve in figure 5 for

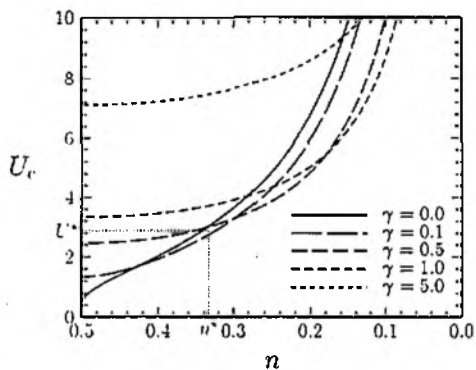


**Figure 5.** Critical interaction against filling for various disorder strengths (zero temperature). A system with filling  $n^*$  and interaction  $U^*$  shows anomalous behaviour with respect to the disorder.

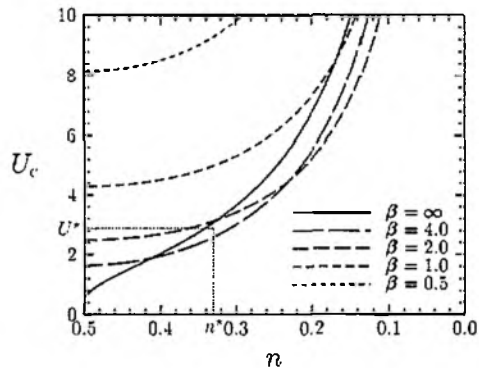


**Figure 6.** Critical interaction against filling for various temperatures (zero disorder). A system with filling  $n^*$  and interaction  $U^*$  shows anomalous behaviour with respect to the temperature.

$\gamma = 0$ . For small (but finite) temperatures the perfect-nesting singularity disappears:  $U_c \sim \pi / [\ln(8\beta/\pi) + C - 1]$ , where  $C \simeq 0.5772$  is Euler's constant [32].

Furthermore, an anomalous behaviour similar to the situation where only disorder was present can be observed. The curves with  $\beta \leq 1$  displayed in figure 6 for different temperature intersects. Thus we introduce the filling  $n_A(\beta)$  at which two  $U_c$  against  $n$  curves intersect which differ only by  $dT$  in the temperature. Thus, by varying  $T \rightarrow T + dT$  at filling  $n < n_A(\beta)$  the critical interaction  $U_c$  decreases, whereas at filling  $n > n_A(\beta)$  an increase of  $U_c$  takes place (see figure 6). The region  $n < n_A(\beta)$  is anomalous because *the temperature fluctuations favour the CDW phase*. The filling  $n_A(\beta)$  separates between the regions of conventional and anomalous behaviour with respect to the temperature. For increasing temperature  $n_A(\beta)$  decreases so that the anomalous region becomes smaller. This will be investigated in appendix A.

To clarify this point we take a specific example with  $n^*, U^*$  as indicated in figure 6. For zero temperature this system is in the homogeneous phase. When the temperature is increased a phase transition takes place and for  $\beta \approx 4$  the system is in the CDW phase. If the temperature is increased further,  $\beta \geq 2$ , the system turns to the homogeneous phase again. The latter is to be expected since, for high enough temperatures, these fluctuations dominate the system.

#### 4.3. Finite temperature and finite disorder

Finally, we have to discuss the situation with finite disorder and finite temperature, i.e.  $\beta \neq \infty$ ,  $\gamma \neq 0$ . For this situation we have to extend the definitions of  $n_A(\gamma)$  and  $n_A(\beta)$  to  $n_A^\beta(\gamma)$  and  $n_A^\gamma(\beta)$ , respectively. The superscript indicates the parameter that is kept constant. In figure 7  $U_c$  curves are given for different values of  $\beta$  and  $\gamma$  (using equation (20)). For legibility  $U_c n$ , rather than  $U_c$  itself, is plotted against  $n$ . In this way the divergence of  $U_c$  for  $n \rightarrow 0$  is compensated. This has the advantage that one can easily detect any intersection since  $U_c n$  is bounded. The number of intersections, and thus the sequence of the curves for fixed filling, is not affected by this type of plot so that conclusions regarding the existence of anomalous behaviour can still be drawn.

Comparison between the figures 5, 6 and 7 shows the following.

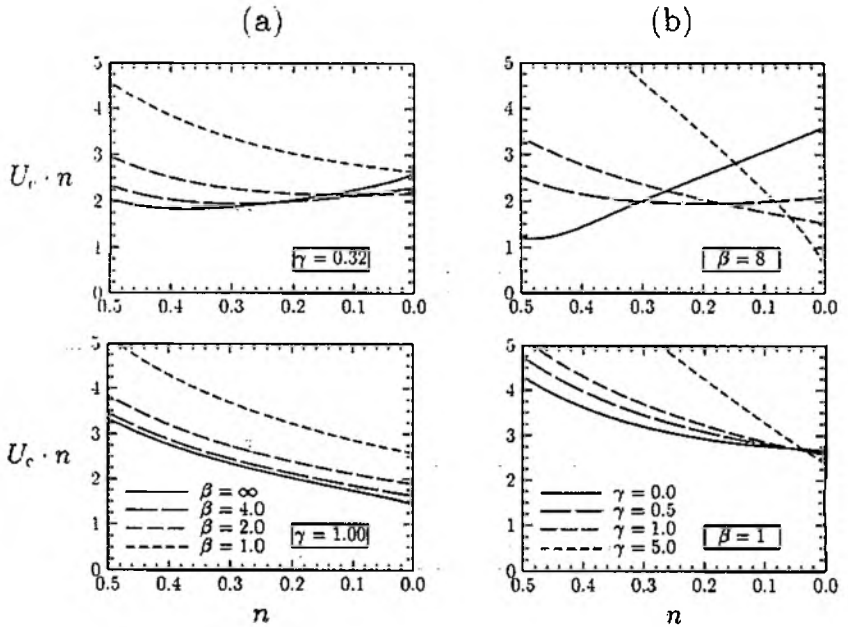


**Figure 7.** Plots displaying the global behaviour of the critical interaction. (a) Fixed disorder at various temperatures, intersections disappear for increasing disorder. (b) Fixed temperature at various disorder strengths. The intersections do not disappear for increasing temperature and shift to the right (empty band).

(i) There exist two particular temperatures  $T_{S1}$  and  $T_{S2}$  (see figures 6 and 7(a)), which are defined by the following properties. The phase transition of a given system at a temperature  $T > T_{S2}$  is conventional. For  $T < T_{S2}$  an anomalous transition is the generic case for low fillings. If the system is such that a phase transition occurs at  $T > T_{S1}$  then the system displays *only* conventional transitions. In figure 8  $T_{S1}$  and  $T_{S2}$  are plotted against the disorder. Note, that general conclusions regarding the temperature  $T < T_{S2}$  or  $T < T_{S1}$  cannot be drawn.

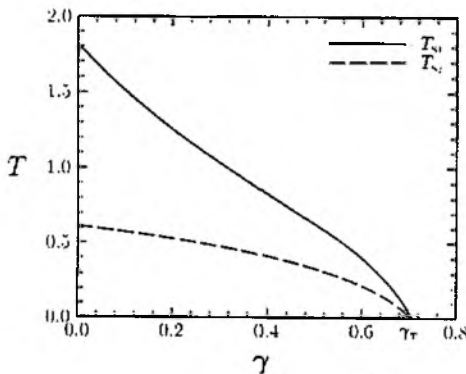


**Figure 8.** The temperatures  $T_{S1}$  and  $T_{S2}$  against the disorder,  $\gamma_T$  is situated where the curves cut the abscissa.

(ii) There exists a special value of the disorder,  $\gamma_T$ , characterized by the disappearance of the anomalous temperature behaviour (see figure 7(b)). For disorder  $\gamma \geq \gamma_T$  the system shows conventional behaviour at all fillings. In figure 8  $\gamma_T$  is the value for which  $T_{S1}$  and  $T_{S2}$  vanish.

(iii) There exists *no* special value of the temperature at which the anomalous disorder effect disappears fully (see figure 7(b)). For increasing temperature the anomalous region decreases but does not vanish.

In appendix A a detailed discussion is presented.

## 5. Physical picture

The anomalous behaviour found in the previous section has a very natural explanation in terms of particle-density fluctuations. In the simplest situation,  $\beta = \infty$ ,  $\gamma = 0$ , the only free parameters are  $n$  and  $U$ . The competition between the potential and the kinetic term in the Hamiltonian (1) allows for a phase transition. It is clear that for low  $U$  (or for low filling, low  $Un$ ) the kinetic energy dominates the system so that it is in the homogeneous phase. For very high  $U$  the potential term dominates, giving rise to a CDW in the entire system. Thus there exists (at least) one critical  $U_c$ .

At zero temperature, disorder has the following influence. At half filling the perfect-nesting singularity disappears because the repulsion must cope with the stochastic fluctuation of the site energies. Therefore,  $U_c$  cannot be zero at half filling. Equivalently, disorder creates regions where higher or lower site energies prevail, so that the density of electrons differs from half filling in these regions. Hence, a higher interaction  $U_c > 0$  is needed to induce the phase transition.

Away from half filling we have the anomalous region  $n < n_A(\gamma)$ . Here the critical interaction  $U_c$  decreases for increasing disorder. The key point is that the regions of higher particle density are now *closer* to half filling. This greatly enhances their tendency towards a phase transition greatly. In the regions of lower particle density the tendency towards a phase transition is weakened but they are surrounded by regions where a CDW is present or easily formed. These regions produce a symmetry-breaking field acting on the surfaces of the regions of lower particle density. The resulting 'proximity' effect eventually stimulates the phase transition in the whole system.

At zero disorder, finite temperatures act, in principle, similarly since they also induce particle density fluctuations which are not present at  $T = 0$  in the ground state (eigenstate of the particle number operator). So it is not surprising that the same behaviour as for disorder is found. Yet there is an important difference: the disorder-induced fluctuations are static whereas the temperature-induced fluctuations are dynamic. This difference is expressed in the existence of the sorting temperatures  $T_{S1}$  and  $T_{S2}$ . They provide evidence that the anomalous temperature behaviour is suppressed at high temperatures. A corresponding suppression of the anomalous disorder behaviour is not observed.

According to the above discussion the combined regime does not produce qualitatively new effects. As long as the fluctuations are weak they push the system into the same direction, hampering the phase transition around half filling and favouring it for lower fillings. The difference between temperature and disorder is revealed in the strong fluctuation regime; the anomalous temperature behaviour is suppressed by strong (dynamic) particle density fluctuations due to temperature.

This effect is enhanced by the presence of (static) disorder fluctuations as can be seen from the monotonic decrease of  $T_{S1}$  and  $T_{S2}$  with increasing disorder  $\gamma$  (see figure 8). In contrast to this, the regime where anomalous disorder behaviour occurs is pushed to lower fillings by high temperature or strong disorder *but* never ceases to exist.

## 6. Critical behaviour of the order parameter

To compute the critical behaviour of the order parameter  $b$  as a function of the interaction  $U$ , the disorder parameter  $\gamma$  and the temperature  $T$ , we use the self-consistency equation (15) and expand it to second order in  $\Delta$ . This shows that in general the critical exponent is  $\frac{1}{2}$ , as can be expected from a mean-field theory. Neither disorder nor temperature alter this fact.

The expansion of (15) yields

$$\frac{1}{U} = \tilde{C}(n, \Delta) = \frac{1}{U_c} + \frac{1}{2} \frac{\partial^2}{\partial \Delta^2} \tilde{C}(n, 0) \Delta^2 + \mathcal{O}(\Delta^4). \quad (23)$$

The important point is the derivation at *constant*  $n$ , which is indicated by the argument of the function  $\tilde{C}(n, \Delta)$  which is the inverse of the right-hand side of (15b). Let  $C(\mu, \Delta)$  be the corresponding function of  $\mu$  and  $n(\mu, \Delta)$ , i.e. the function for the particle number at given chemical potential. Both  $C(\mu, \Delta)$  and  $\tilde{C}(n, \Delta)$  depend only on the modulus of  $\Delta$ . The sign of  $\Delta$  is of no importance in (15b). Then  $\frac{\partial^2}{\partial \Delta^2} \tilde{C}(n, 0)$  is given by

$$\frac{\partial^2}{\partial \Delta^2} \tilde{C}(n, 0) = \frac{\partial^2}{\partial \Delta^2} C(\mu, 0) - \left( \frac{\partial^2}{\partial \Delta^2} n(\mu, 0) \right) \left( \frac{\partial}{\partial \mu} C(\mu, 0) \right) \left( \frac{\partial}{\partial \mu} n(\mu, 0) \right)^{-1}. \quad (24)$$

In order to calculate the quantities introduced above we have to know the Green function  $g_L(z, \Delta)$  up to third order in  $\Delta$ , where  $z$  is a complex energy. The derivatives of  $g_L(z, \Delta)$  at  $\Delta = 0$  can be calculated by repeated derivation of (14) and the use of  $g_L(z, \Delta) = g_U(z, -\Delta)$ . This task is straightforward. The intermediate steps are given in appendix B.

For the following it is important to know that  $\frac{\partial^2}{\partial \Delta^2} \tilde{C}(n, 0)$  exists. It is negative, which is necessary for the expansion to be meaningful. The only exception is half filling ( $\mu = 0$ ), zero disorder ( $\gamma = 0$ ), and zero temperature ( $T = 0$ ). In this case  $\frac{\partial^2}{\partial \Delta^2} \tilde{C}(n, 0)$  diverges and the expansion (23) breaks down. This case will be investigated separately in the following section.

### 6.1. Critical interaction

For finite  $U_c$ , which is the generic case, equation (23) or equivalently

$$b = \frac{1}{U} \left( \frac{2/U - 2/U_c}{\partial^2 \tilde{C}(n, 0) / \partial \Delta^2} \right)^{1/2} \quad (25)$$

implies

$$b \propto \sqrt{U - U_c}. \quad (26)$$

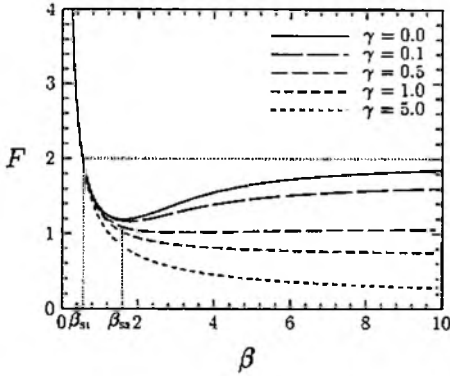


**Figure 9.** Order parameter  $b(\beta, \gamma_0)$  against temperature  $T$  at fixed disorder  $\gamma_0 = 0.01$  and filling  $n = 0.45$  for different values of the interaction  $U$ : (a)  $U > U_c(\infty, \gamma_0)$ ; (b)  $U = U_c(\infty, \gamma_0)$ , (c)  $U < U_c(\infty, \gamma_0)$ .

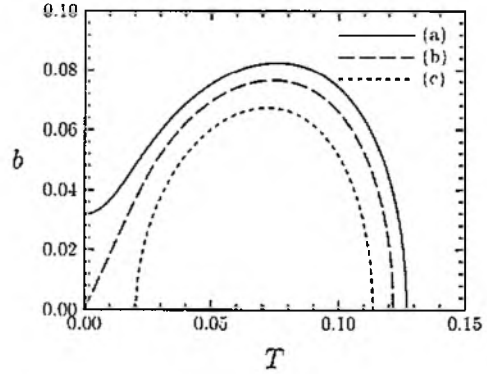


**Figure 10.** Order parameter  $b(\beta_0, \gamma)$  against disorder  $\sqrt{\gamma}$  at fixed temperature  $\beta_0 = 100$  and filling  $n = 0.45$  for different values of the interaction  $U$ : (a)  $U > U_c(\beta_0, 0)$ ; (b)  $U = U_c(\beta_0, 0)$ , (c)  $U < U_c(\beta_0, 0)$ .

So  $b$ , as a function of the next-neighbour interaction  $U$ , has the critical exponent  $\frac{1}{2}$  in infinite dimensions. The only exception to this result occurs for  $U_c = 0$  at zero temperature, zero disorder and half filling, i.e.  $\mu = 0$ . In this case we resort to (15) and (17):

$$\Delta = \frac{U\Delta}{2\pi} \int_{\Delta}^{\sqrt{4+\Delta^2}} d\omega \left( \frac{4 + \Delta^2 - \omega^2}{\omega^2 - \Delta^2} \right)^{1/2} \quad (27)$$

which yields  $\Delta \approx (U\Delta/\pi)[- \ln(\Delta/8) - 1]$  in the regime of small  $\Delta$ . In this case we obtain for the critical behaviour

$$b = \frac{8}{U} \exp\left(-\frac{\pi}{U} - 1\right). \quad (28)$$

This is the generic result for  $U_c = 0$  in Hartree-Fock theory as is shown in a general framework by Uhrig *et al* [33].

## 6.2. Critical temperatures

We now address the critical behaviour of the order parameter  $b(\beta, \gamma_0)$  as a function of the temperature  $T$  at fixed disorder  $\gamma_0$ . Our numerical work shows that there are three types of global behaviour of  $b(\beta, \gamma_0)$  at constant filling (see figure 9). Curve (c) in figure 9 has two critical temperatures: one is conventional ( $T_N$ ) because  $b(\beta, \gamma_0) = 0$  for  $T \geq T_N$  and the other is anomalous because  $b(\beta, \gamma_0) = 0$  for  $T \leq T_A$ . The necessary but not sufficient condition for this phenomenon is  $U < U_c(\infty, \gamma_0)$ . Curve (a) in figure 9 shows only one conventional critical temperature; the curve is characterized by  $U > U_c(\infty, \gamma_0)$ . Curve (b) in figure 9 marks the transition between curve (a) and (c) in the same figure for  $U = U_c(\infty, \gamma_0)$ . Since all functions on the right-hand side of (25) are differentiable in the temperature at finite temperature, we have  $\Delta \propto \sqrt{T_N - T}$  and  $\Delta \propto \sqrt{T - T_A}$  for  $T_A > 0$ . Only in curve (b) of figure 9 for  $T_A = 0$  we obtain a linear behaviour  $\Delta \propto T$  because the low temperature expansion of  $1/U_c$  contains only even powers of  $T$ .

To conclude the discussion of the anomalous temperature dependence we state a necessary condition for its occurrence

$$|n - \frac{1}{2}| \geq |n_{\Lambda}^{\gamma}(\infty) - \frac{1}{2}| \geq \frac{1}{\pi} \left[ \frac{\gamma}{1 - \gamma^2} \sqrt{1 - 2\gamma^2} + \sin^{-1} \left( \frac{\gamma}{\sqrt{1 - \gamma^2}} \right) \right]. \quad (29)$$

This can be deduced from  $\partial/\partial(T^2)|_{n,\gamma}[U_c]^{-1}(\infty, \gamma_0) > 0$ . At first sight (29) is only valid at  $\beta = \infty$ , i.e. for curve (b) in figure 9. But (29) can be extended to general temperatures since curves (b) and (c) in figure 9 differ only in their value of  $U$ . In other words: to each curve of type (c) corresponds one of type (b). This statement is true taking for granted that there are *no* curves with three or more critical temperatures, which is supported by our numerical calculations.

Condition (29) is also the sufficient condition for the occurrence of anomalous temperature dependence when we permit to choose the value of the interaction  $U$  suitably, i.e.  $U < U_c(\infty, \gamma_0)$  but not too small either. Otherwise no region of finite-order parameter will be found. Furthermore, condition (29) tells us that there is a special value of disorder  $\gamma_T = 1/\sqrt{2}$  above which *no* anomalous temperature dependence is possible because (29) can no longer be fulfilled. This phenomenon has already been found in section 4.3.

### 6.3. Critical disorders

The discussion of  $b(\beta_0, \gamma)$ , for constant temperature, is quite analogous to that of  $b(\beta, \gamma_0)$ . It is appropriate to stress the similarity by focusing on  $b(\beta_0, \gamma)$  against  $\sqrt{\gamma}$  rather than on  $b(\beta_0, \gamma)$  against  $\gamma$  because  $\sqrt{\gamma}$  is an energy as is  $T$ . The three generic types of curves  $b(\beta_0, \gamma)$  at constant filling are shown in figure 10. Curve (a) in figure 10 with  $U > U_c(\beta_0, 0)$  displays one conventional critical disorder  $\gamma_C$ ; curve (c) in figure 10 with  $U < U_c(\beta_0, 0)$  has two critical disorder values one of which is conventional, the other anomalous:  $\gamma_C > \gamma_A$ . Curve (b) in figure 10 marks the special case  $U = U_c(\beta_0, 0)$ . For the conventional critical disorders we again find  $b \propto \sqrt{\gamma_C - \gamma}$  and for the anomalous disorder  $\gamma_A > 0$  we have  $b \propto \sqrt{\gamma - \gamma_C}$ . For curve (c) in figure 10 with  $\gamma_A = 0$  we obtain  $b \propto \sqrt{\gamma}$  which stresses the similarity between  $\sqrt{\gamma}$  and the temperature  $T$  as stated at the beginning of this section. All these statements follow from the differentiability of  $1/U_c(\beta_0, \gamma)$  for  $U_c \neq 0$  given equation (25).

As in the previous section a necessary and sufficient condition for the occurrence of anomalous behaviour can be given as

$$\frac{\partial}{\partial \gamma} \left|_{n,\beta} \frac{1}{U_c(\beta, \gamma)} \right|_{\gamma=0} > 0. \quad (30)$$

This is, however, more complicated to evaluate and we do not give its explicit form. In analogy with the argument in section 6.2, the infinitesimal validity of (30) is globally extended by the fact that to each curve of type (c) corresponds a curve of type (b) in figure 10. This observation makes (30) even a sufficient condition for the appearance of anomalous behaviour at certain values of the interaction  $U$ .

After pointing out the similarities between temperature and disorder one important difference must be emphasized. Whereas there exists a certain disorder  $\gamma_T$  above which any temperature anomaly ceases to exist there is *no* temperature above which the disorder anomaly will vanish for all fillings. This is shown by the high-temperature expansion of the divergence strength in appendix A.

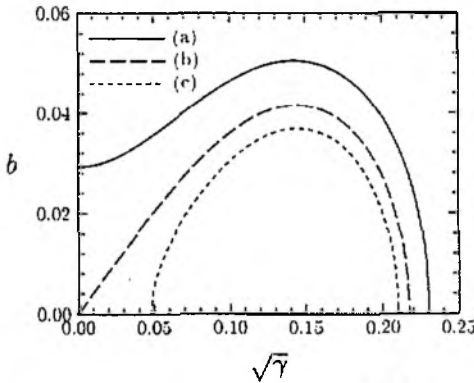


**Figure 11.** Divergence coefficient  $F(\beta, \gamma)$  against inverse temperature. The curves do not intersect. The minimum of each curve is at  $\beta_{S2}$  and the inverse temperature  $\beta_{S1}$  is given at the intersection of the curve with the asymptote for  $\beta \rightarrow \infty$ .

## 7. Discussion

In this paper we have obtained the exact solution for a model of spinless fermions with nearest neighbour interaction and local disorder on a Bethe lattice with infinite coordination number. An essential aspect of this solution is the decomposition of the self-energy into two separate parts. We have shown, at least in this explicit example, that the limit of large coordination numbers  $Z \rightarrow \infty$  makes possible the formulation of a self-consistent mean-field theory for interacting disordered fermions.

We chose to work on a Bethe lattice for mathematical convenience. Our method is equally applicable to any lattice which can be generalized to infinite coordination numbers. The Bethe lattice is bipartite, as is the hypercubic lattice. For the one-particle properties only, the local surrounding of a given site is of importance so that their differences on the hypercubic and on the Bethe lattice are only quantitative. Moreover, in the limit  $Z \rightarrow \infty$  the Bethe lattice has the advantage that its bandwidth remains finite whereas in the hypercubic case the bandwidth diverges. In spite of these greatly simplifying features the phase diagram was found to have a significant unusual structure.

In the model of spinless fermions the homogeneous phase becomes unstable at a critical interaction and a phase transition occurs. We extensively discussed the dependence of this transition on the external parameters, i.e. interaction strength, disorder, temperature and filling. Our main findings are the following.

(i) The perfect-nesting singularity is suppressed by disorder and/or temperature.

(ii) The system shows anomalous behaviour away from half filling, i.e. the tendency towards spontaneous symmetry breaking is enhanced by weak disorder and/or low temperature.

The above phenomena can be explained in terms of static (for disorder) and dynamic (for temperature) particle-density fluctuations. They drive the system away from half filling in the former case and bring it closer to half filling in the latter.

Although the model of spinless fermions is considerably simpler than the Hubbard model, there do exist qualitative similarities between the features of our exact solution for  $Z \rightarrow \infty$  and those of approximate treatments of the Hubbard model. For example, using a  $t^2/U$  expansion Khomskii [34] finds an anomalous temperature behaviour

regarding the antiferromagnetic phase away from half filling. At half filling the corresponding order parameter decreases with increasing temperature. In the same limit Zimanyi and Abrahams [11] noted that the Mott insulating region around half filling is widened by the effect of disorder on the interaction and that the critical temperature  $T_c$  may be increased by disorder. Lee and Ramakrishnan argue that disorder enhances the effects of the interaction because it renders the electron motion diffusive [1]. Our model gives a possibility to study the disorder-induced enhancement quantitatively and in a controlled approximation.

The present treatment can be extended in several directions. While the use of the Bethe lattice in combination with infinite branching has proved to be very useful for the calculation of one-particle properties, it is not adequate for the description of two-particle properties such as transport coefficients and requires a suitable generalization. This problem and its possible solution will be the subject of subsequent publication in which the role of diffusive motion as proposed by Lee and Ramakrishnan [1] will also be investigated.

Since the mean-field theory is controlled by the small expansion parameter  $1/Z$  it can be extended by including self-consistent  $1/Z$  corrections. The effects of quantum mechanical fluctuations on the phase transition, the phenomenon of Anderson localization and the influence of interaction on it, and so on, should then be accessible. As a first step, however, the separate problems, i.e. disorder or interaction, must be solved with  $1/Z$  corrections.

## Acknowledgments

We would like to thank Dr V Janiš and Dipl. Phys. R Strack for valuable discussions. This work was supported in part by the SFB 341 of the Deutsche Forschungsgemeinschaft. One of us (GU) gratefully acknowledges the support of the Studienstiftung des Deutschen Volkes.

## Appendix A.

In this appendix we discuss the temperatures  $T_{S1}$ ,  $T_{S2}$ , the disorder  $\gamma_T$  and the fillings  $n_A^\beta(\gamma)$ ,  $n_A^\gamma(\beta)$ , introduced in section 4.3. All critical interaction curves in figure 5 and figure 6 diverge at the empty band limit with  $U_c \propto n^{-1}$ . This can be seen from equation (20). Expansion of  $n(\beta, \gamma)$  and  $[U_c(\beta, \gamma)]^{-1}$  at the appropriate  $\mu$  gives the same leading coefficient.

From figure 7 we learn that, for increasing temperature and/or disorder,  $n_A^\beta(\gamma)$  and  $n_A^\gamma(\beta)$  approach zero. The quantities  $\beta_{S1} = T_{S1}^{-1}$ ,  $\beta_{S2} = T_{S2}^{-1}$  and  $\gamma_T$  are therefore determined by the behaviour of the system at low filling. This observation makes it possible to expand (20) around  $\mu = -2\sqrt{\gamma+1}$  for  $\beta = \infty$  and around  $\mu \rightarrow -\infty$  for  $\beta < \infty$ . Since  $U_c \propto n^{-1}$  it is helpful to introduce the 'divergence coefficient'  $F(\beta, \gamma)$  as:

$$F(\beta, \gamma) = n(\beta, \gamma)U_c(\beta, \gamma). \quad (A1)$$

This quantity is plotted in figure 7. Asymptotic expansion gives

$$F(\beta, \gamma) = \begin{cases} [2/(\gamma + 1)^{3/2}]\{1 + \frac{3}{4}[(2\gamma^2 - 1)/\sqrt{\gamma + 1}]\beta^{-1} + \mathcal{O}(\beta^{-2})\} & \beta \rightarrow \infty \\ (1/\beta)[1 + \frac{1}{2}\beta^2 + \frac{1}{90}\beta^4(1 - 6\gamma) + \mathcal{O}(\beta^6)] & \beta \rightarrow 0. \end{cases} \quad (\text{A2})$$

Expansion at zero temperature gives  $F(\infty, \gamma) = 2(\gamma + 1)^{-3/2}$  which is in accordance with (A2). In figure 11  $F(\beta, \gamma)$  is plotted against  $\beta$  for several values of the disorder. It is important to recognize that the curves in figure 11 do *not* intersect. For temperatures  $1 < \beta < 10$  this is seen directly from figure 11; for high temperatures, we obtain from (A2)  $\frac{\partial F}{\partial \gamma}|_{\beta \rightarrow 0} = -\frac{1}{15}\beta^3 < 0$  and for low/zero temperatures  $\frac{\partial F}{\partial \gamma}|_{\beta \rightarrow \infty} = -3(\gamma + 1)^{-5/2} < 0$ . This implies that, in the limit of low filling  $\frac{\partial U_c}{\partial \gamma}|_{n=0} < 0$ , whereas  $\frac{\partial U_c}{\partial \gamma}|_{n=1/2} > 0$ . Thus there must be at least one intersection between each  $U_c(\beta, \gamma_1)$  and  $U_c(\beta, \gamma_2)$  where  $\gamma_1 \neq \gamma_2$ , and so there exists no temperature analog to  $\gamma_T$ . This is valid at all temperatures.

From figure 11 one can also extract information regarding  $\beta_{S1}$  and  $\beta_{S2}$ . Both are indicated (figure 11) for zero disorder, and can be found from  $F(\beta_{S1}, \gamma) = F(\infty, \gamma)$  and  $\frac{\partial F}{\partial \beta}(\beta_{S2}, \gamma) = 0$ , respectively. This leads to

$$\int_{-2\sqrt{\gamma+1}}^{2\sqrt{\gamma+1}} d\omega \left( \frac{\sqrt{\gamma+1}[(\gamma-1)\omega^2 - 4\gamma^2] - 4\omega}{(\gamma-1)\omega^2 - 4\gamma^2} \right) \sqrt{4(\gamma+1) - \omega^2} \exp(-\beta_{S1}\omega) = 0 \quad (\text{A3})$$

from which  $\beta_{S1}$  can be extracted and

$$\int_{-2\sqrt{\gamma+1}}^{2\sqrt{\gamma+1}} d\omega \left[ 2\sqrt{\gamma+1} I_2(2\beta_{S2}\sqrt{\gamma+1}) + \omega I_1(2\beta_{S2}\sqrt{\gamma+1}) \right] \times \frac{\omega \sqrt{4(\gamma+1) - \omega^2}}{(\gamma-1)\omega^2 - 4\gamma^2} \exp(-\beta_{S2}\omega) = 0 \quad (\text{A4})$$

from which  $\beta_{S2}$  can be determined. Here  $I_1$  and  $I_2$  are Bessel functions [32].

It remains to calculate  $\gamma_T$ , the disorder strength above which the anomalous temperature behaviour ceases to exist. This is the case when  $\beta_{S2} \rightarrow \infty$ . Thus  $\gamma_T$  is defined as

$$\lim_{\beta \rightarrow \infty} \beta^2 \frac{\partial F(\beta, \gamma_T)}{\partial \beta} = 0. \quad (\text{A5})$$

To find the corresponding disorder we make use of (A2) and find  $\gamma_T = \frac{1}{2}\sqrt{2}$ . The same result can be obtained for general filling as shown in section 6.2.

## Appendix B.

To find the critical behaviour of the order parameter in section 6 the derivatives of the Green function  $g_L$  must be calculated. Here we give the results for the corresponding

densities  $\rho_L^{(n)}(\omega)$

$$\rho_L(\omega) = \frac{1}{2\pi(1+\gamma)} \sqrt{4(1+\gamma) - \omega^2} \quad (\text{B1a})$$

$$\rho_L^{(1)}(\omega) = -\frac{1}{2\pi} \frac{\omega \sqrt{4(1+\gamma) - \omega^2}}{4\gamma^2 + (1-\gamma)\omega^2} \quad (\text{B1b})$$

$$\rho_L^{(2)}(\omega) = \frac{2}{\pi} \frac{\omega^2(1+\gamma^2) - 4\gamma^2(1+\gamma)}{(4\gamma^2 + (1-\gamma)\omega^2)^2 \sqrt{4(1+\gamma) - \omega^2}} \quad (\text{B1c})$$

$$\rho_L^{(3)}(\omega) = \frac{-6\omega}{\pi(1-\gamma)^2 \sqrt{4(1+\gamma) - \omega^2}} \left( \frac{2^7 \gamma^4}{(4\gamma^2 + (1-\gamma)\omega^2)^4} - \frac{2^5 \gamma^2(1+\gamma^2)}{(4\gamma^2 + (1-\gamma)\omega^2)^3} + \frac{\gamma^4 + 6\gamma^2 + 1}{(4\gamma^2 + (1-\gamma)\omega^2)^2} \right) \quad (\text{B1d})$$

where  $\omega \in [-2\sqrt{1+\gamma}, 2\sqrt{1+\gamma}]$ . The superscript ( $n$ ) stands for the  $n$ th derivative with respect to  $\Delta$ . The densities of (B1) have to be integrated to give the functions which enter in (24). To this end we define

$$R^{(n)}(\mu) := \int_{-2\sqrt{1+\gamma}}^{\mu} d\omega \rho_L^{(n)}(\omega). \quad (\text{B2})$$

Once we know  $\rho_L^{(n)}(\mu)$  and  $R^{(n)}(\mu)$  the functions

$$\frac{\partial}{\partial \mu} n(\mu, 0) = \rho_L(\mu) \quad (\text{B3a})$$

$$\frac{\partial^2}{\partial \Delta^2} n(\mu, 0) = R^{(2)}(\mu) \quad (\text{B3b})$$

$$\frac{\partial}{\partial \mu} C(\mu, 0) = \rho_L^{(1)}(\mu) \quad (\text{B3c})$$

$$\frac{\partial^2}{\partial \Delta^2} C(\mu, 0) = \frac{1}{3} R^{(3)}(\mu) \quad (\text{B3d})$$

for  $\beta = \infty$  are given.

The factor  $\frac{1}{3}$  in the last equation arises from the Taylor series expansion. For completeness we also state the explicit forms of  $R^{(2)}(\mu)$  and  $R^{(3)}(\mu)$ :

$$R^{(2)}(\mu) = -\frac{1}{2\pi} \frac{\mu \sqrt{4(1+\gamma) - \mu^2}}{4\gamma^2 + (1-\gamma)\mu^2} \quad (\text{B4a})$$

$$R^{(3)}(\mu) = \frac{\sqrt{4(1+\gamma) - \mu^2}}{8\pi(1-\gamma)^2} \left( 3H_2(\mu, \gamma) + \frac{6}{4\gamma^2 + (1-\gamma)\mu^2} - 2^4 \frac{\gamma^4 + 6\gamma^2}{(4\gamma^2 + (1-\gamma)\mu^2)^2} + 2^8 \frac{\gamma^4}{(4\gamma^2 + (1-\gamma)\mu^2)^3} \right) \quad (\text{B4b})$$

where

$$H_2(\mu, \gamma) := \begin{cases} (1/2h) \ln[(2+h)/(2-h)] & \gamma < 1 \\ \frac{1}{2} & \gamma = 1 \\ (1/h) \tan^{-1}(\frac{1}{2}h) & \gamma > 1 \end{cases} \quad (\text{B5a})$$

$$h := \sqrt{|1-\gamma|(4(1+\gamma) - \mu^2)}. \quad (\text{B5b})$$

In principle (B3) also provides the necessary information for the calculation of the corresponding functions at finite temperature. To obtain finite-temperature results the right-hand sides of (B3) have to be convoluted with the temperature peak, i.e. the negative derivative of the Fermi function. Thus it is not straightforward to obtain  $\frac{\partial^2}{\partial \Delta^2} \tilde{C}(n, 0)$  at finite temperatures since several convolutions are involved. Yet it is easy to compute  $\frac{\partial^2}{\partial \Delta^2} \tilde{C}(n, 0)$  at zero temperature ( $\beta = \infty$ ):

$$\begin{aligned} \frac{\partial^2}{\partial \Delta^2} \tilde{C}(n, 0) = & \frac{\sqrt{4(1+\gamma) - \mu^2}}{24\pi(1-\gamma)^2} \left( 3H_2(\mu, \gamma) + 6 \frac{2\gamma^2 - 1}{4\gamma^2 + (1-\gamma)\mu^2} \right. \\ & \left. - 2^4 \frac{4\gamma^4 + 3\gamma^2}{(4\gamma^2 + (1-\gamma)\mu^2)^2} + 2^8 \frac{\gamma^4}{(4\gamma^2 + (1-\gamma)\mu^2)^3} \right) \end{aligned} \quad (\text{B6})$$

and for  $\gamma = 1$  we find

$$\frac{\partial^2}{\partial \Delta^2} \tilde{C}(n, 0) = -\frac{(8 - \mu^2)^{3/2}}{240\pi} (1 + 3\mu^2). \quad (\text{B7})$$

Note the divergence of  $\frac{\partial^2}{\partial \Delta^2} \tilde{C}(n, 0)$  at  $\mu = 0, \gamma = 0$  and  $T = 0$ . The sign of  $\frac{\partial^2}{\partial \Delta^2} \tilde{C}(n, 0)$  is important: it should be negative for the expansion to be meaningful. For  $\gamma = 1$  this is clear from (B7). For the other values of disorder  $\gamma \geq 0$  and chemical potential  $\mu \in (-2\sqrt{1+\gamma}, 2\sqrt{1+\gamma})$  at zero temperature this can be shown rigorously by using the inequalities

$$\frac{1}{2x} \ln \left( \frac{1+x}{1-x} \right) < \frac{1}{3} \left( 2 + \frac{1}{1-x^2} \right) \quad x \in (0, 1) \quad (\text{B8a})$$

$$\frac{1}{x} \tan^{-1}(x) < \frac{1}{3} \left( 2 + \frac{1}{1+x^2} \right) \quad x > 0. \quad (\text{B8b})$$

For finite temperatures we verified numerically that  $\frac{\partial^2}{\partial \Delta^2} \tilde{C}(n, 0)$  has the correct sign and does not vanish.

## References

- [1] Lee P A and Ramakrishnan T V 1985 *Rev. Mod. Phys.* **57** 287
- [2] Wegner F J 1979 *Z. Phys.* **B 35** 207
- [3] Finkel'shtein A M 1983 *Sov. Phys.-JETP* **57** 97
- [4] Castellani C, Di Castro C, Lee P A and Ma M 1984 *Phys. Rev.* **B 30** 527  
Castellani C, Di Castro C and Grilli M 1986 *Phys. Rev.* **B 34** 5907
- [5] Finkel'shtein A M 1984 *Z. Phys.* **B 56** 189

- [6] Castellani C, Di Castro C, Lee P A, Ma M, Sorella S and Tabet E 1984 *Phys. Rev. B* **30** 1596
- Castellani C, Di Castro C, Lee P A, Ma M, Sorella S and Tabet E 1986 *Phys. Rev. B* **33** 6169
- [7] Castellani C, Kotliar G and Lee P A 1987 *Phys. Rev. Lett.* **59** 323
- [8] Belitz D and Kirkpatrick T R 1990 *Physica A* **167** 259
- [9] Milovanović M, Sachdev S and Bhatt R N 1989 *Phys. Rev. Lett.* **63** 82
- [10] Ma M 1982 *Phys. Rev. B* **26** 5097
- [11] Zimanyi G T and Abrahams E 1990 *Phys. Rev. Lett.* **22** 2719
- [12] Metzner W and Vollhardt D 1989 *Phys. Rev. Lett.* **62** 324
- [13] Vollhardt D 1990 *Physica B* **169** 277
- Vollhardt D 1992 *Correlated Electron Systems* ed V J Emery (Singapore: World Scientific) at press
- [14] Müller-Hartmann E 1989 *Int. J. Mod. Phys. B* **3** 2169
- [15] Vlaming R and Vollhardt D 1992 *Phys. Rev. B* **45** 4637
- [16] Müller-Hartmann E 1989 *Z. Phys. B* **74** 507
- [17] Janiš V 1991 *Z. Phys. B* **83** 227
- [18] George A and Kotliar G 1992 *Phys. Rev. B* **45** 6479
- [19] Janiš V and Vollhardt D 1992 *Int. J. Mod. Phys. B* **6** 6731
- [20] Tsuda N, Nasu K, Yanase A and Sitatori K 1991 *Electronic Conduction in Oxides* (Berlin: Springer)
- [21] Cullen J R and Callen E 1970 *J. Appl. Phys.* **41** 879
- [22] Cullen J R and Callen E 1971 *J. Phys.* **26** 236
- [23] des Cloizeaux J and Gaudin M 1966 *J. Math. Phys.* **7** 1384
- [24] Yang C N and Yang C P 1966 *Phys. Rev.* **150** 321, 327
- [25] Fazekas P 1972 *Solid State Commun.* **10** 175
- [26] Shankar R 1990 *Int. J. Mod. Phys. B* **4** 2371
- [27] Shankar R 1991 *Physica A* **177** 530
- [28] White C T and Economou E N 1977 *Phys. Rev. B* **8** 3742
- [29] Economou E N 1979 *Green's Functions in Quantum Physics* (Berlin: Springer)
- [30] Mahan G D 1990 *Many Particle Physics* (New York: Plenum) 2nd edn
- [31] Rickayzen G 1980 *Green's Functions and Condensed Matter* (London: Academic)
- [32] Abramowitz M and Stegun I A 1964 *Handbook of Mathematical Functions* (New York: Dover)
- [33] Uhrig G S, Strack R and Vollhardt D 1992 *Phys. Rev. B* at press
- [34] Khomskii D I 1970 *Phys. Metals Metallography* **29** 31